

9-24-2007

Enhancement of Nd: YAG LIBS Emission of a Remote Target Using a Simultaneous CO/sub 2/ Laser Pulse

Dennis K. Killinger
University of South Florida

Susan D. Allen
Arkansas State University - Main Campus, allens17@erau.edu

Robert D. Waterbury
Alakai, Inc.

Chris Stefano
Alakai, Inc.

Edwin L. Dottery
Alakai, Inc.

Follow this and additional works at: <https://commons.erau.edu/publication>

 Part of the [Physical Sciences and Mathematics Commons](#)

Scholarly Commons Citation

Killinger, D. K., Allen, S. D., Waterbury, R. D., Stefano, C., & Dottery, E. L. (2007). Enhancement of Nd: YAG LIBS Emission of a Remote Target Using a Simultaneous CO/sub 2/ Laser Pulse. *Optics Express*, 15(20). <https://doi.org/10.1364/OE.15.012905>

This Article is brought to you for free and open access by Scholarly Commons. It has been accepted for inclusion in Publications by an authorized administrator of Scholarly Commons. For more information, please contact commons@erau.edu, wolfe309@erau.edu.

Enhancement of Nd:YAG LIBS emission of a remote target using a simultaneous CO₂ laser pulse

Dennis K. Killinger^{1*}, Susan D. Allen², Robert D. Waterbury³, Chris Stefano³, and Edwin L. Dottery³

¹ University of South Florida, 4202 E. Fowler, Tampa, FL 33620

² Arkansas State University, State University, AR 72467

³ Alakai Inc., 7887 Bryan Dairy Rd, Largo, FL 33777

*Corresponding author: killinge@cas.usf.edu

Abstract: For the first time to the best of our knowledge, a simultaneous 10.6 μm CO₂ laser pulse has been used to enhance the Laser Induced Breakdown Spectroscopy (LIBS) emission from a 1.064 μm Nd:YAG laser induced plasma on a hard target. The enhancement factor was on the order of 25 to 300 times, depending upon the emission lines observed. For an alumina ceramic substrate the Al emission lines at 308 nm and Fe impurity line at 278 nm showed an increase of 60x and 119x, respectively. The output energy of the Nd:YAG laser was 50 mJ/pulse focused to a 1 mm diameter spot to produce breakdown. The CO₂ laser pulse had a similar energy density of 40 mJ/mm². Timing overlap of the two laser pulses within 1 microsecond was important for enhancement to be observed. An observed feature was the differential enhancement between different elemental species and also between different ionization states, which may be helpful in the application of LIBS for multi-element analysis.

© 2007 Optical Society of America

OCIS codes: (300.6365) Spectroscopy, laser induced breakdown

References and links

1. K. Song, Y. I. Lee, and J. Sneddon, "Applications of laser-induced breakdown spectrometry," *Appl. Spectrosc. Rev.* **32**, 183-235 (1997).
2. L. J. Radziemski and D. A. Cremers, "Spectrochemical analysis using laser plasma excitation," L. J. Radziemski and D. A. Cremers, eds., in *Laser-Induced Plasma: Physical, Chemical and Biological Applications*, (Marcel Dekker, New York, 1989).
3. A. Miziolek, V. Palleschi, and I. Schechter, eds., *Laser Induced Breakdown Spectroscopy*, (Cambridge University Press 2006).
4. C. Lopez-Moreno, S. Palanco, J. J. Laserna, F. DeLucia Jr., A. W. Miziolek, J. Rose, R. A. Walters, and A. I. Whitehouse, "Test of a stand-off laser-induced-breakdown spectroscopy sensor for the detection of explosive residues on solid surfaces," *J. Anal. At. Spectrom.* **21**, 55 (2006).
5. D. N. Stratis, K. L. Eland, and S. M. Angel, "Enhancement of aluminum, titanium, and iron in glass using pre-ablation spark dual-pulse LIBS," *Appl. Spectrosc.* **54**, 1719 (2000).
6. J. Scaffidi, W. Pearman, J. C. Carter, and S. M. Angel, "Observations in collinear femtosecond-nanosecond dual-pulse laser-induced breakdown spectroscopy," *Appl. Spectrosc.* **60**, 65 (2006).
7. J. Scaffidi, J. Pender, W. Pearman, S. R. Goode, B. W. Colston, Jr., J. C. Carter, and S. M. Angel, "Dual-pulse laser-induced breakdown spectroscopy with combinations of femtosecond and nanosecond laser pulses," *Appl. Opt.* **42**, 6099 (2003).
8. J. Gonzalez, C. Y. Liu, J. H. Yoo, X. L. Mao, and R. E. Russo, "Double-pulse laser ablation ICP-MS and LIBS," *Spectrochim. Acta.* **60**, 27 (2005).
9. V. I. Babushok, F. C. DeLucia Jr., J. L. Gottfried, C. A. Munson, and A. W. Miziolek, "Double pulse laser ablation and plasma: Laser induced breakdown spectroscopy signal enhancement," *Spectrochimica Acta Part B-Atomic Spectrosc.* **61**, 999 (2006).
10. P. Mukherjee, S. Chen, and S. Witanachchi, "Effect of initial plasma geometry and temperature on dynamic expansion in dual-laser ablation," *Appl. Phys. Lett.* **74**, 1546 (1999).

11. K. Song, Y. Lee, and J. Sneddon, "Recent developments in instrumentation for laser induced breakdown spectroscopy," *Appl. Spectrosc. Rev.* **37**, 89 (2002).
 12. S. Y. Chan and N. H. Cheung, "Analysis of solids by laser ablation and resonance-enhanced laser-induced spectroscopy," *Anal. Chem.* **72**, 2087 (2000).
 13. CRC Handbook of Chemistry and Physics, Table of Atomic Spectra (2004).
 14. V. N. Rai, F. Y. Yueh, and J. P. Singh, "Optical emission from laser-produced chromium and magnesium plasma under the effect of two sequential laser pulses," *Pramana-J. of Phys.* **65**, 1075 (2005).
 15. A. G. Leonov, D. I. Chekhov, and A. N. Staristin, "Mechanisms of resonant laser ionization," *J. Exp. Theor. Phys.* **84**, 703 (1997).
 16. J. S. Townsend, *Electricity in Gases*, (Oxford University Press, New York, 1914); reprinted Wexford College Press (2007).
 17. J. Rahel, M. Sira, P. Stahel, and D. Trunec, "The transition between different discharge regimes in atmospheric pressure air barrier discharge," *Contrib. Plasma Phys.* **47**, 34 (2007).
 18. N. Jidenko, C. Jimenez, F. Massines, and J.P. Borra, "Nano-particle size-dependent charging and electro-deposition in dielectric barrier discharges at atmospheric pressure for thin SiO_x film deposition," *J. Phys. D* **40**, 4155 (2007).
-

1. Introduction and background

Laser-Induced-Breakdown Spectroscopy (LIBS) is a recognized laser detection technique for sensing the chemical composition of a wide range of materials including minerals, chemical substances, and trace species [1-3]. Recently, LIBS is being studied for the remote detection of a wide variety of substances such as surface contaminants and other trace materials [4]. There is a need to increase the detection range of such standoff LIBS systems, and, as a result, the need to increase the strength of the LIBS signal.

Toward this end, the work presented in the paper is the first demonstration of significant enhancement of a LIBS emission by several orders of magnitude using a simultaneous CO₂ laser pulse to enhance the initial Nd:YAG induced LIBS plasma emission. We found that enhancements on the order of 25 to 300 could be obtained for the LIBS emission from ceramic (alumina) targets. Laser pulse energy density on target was about 50 mJ/mm² for both lasers, with LIBS emission depending upon both the Nd:YAG and the CO₂ laser pulse intensities. We have also studied the overlap dependence of the two laser pulses and found that the CO₂ laser pulse needs to be simultaneous with the plasma formed (on the order of the pulse width of the CO₂ laser). While additional studies need to be conducted to better quantify the effects of laser beam mode, temporal pulse shaping, individual emission line ionization states, and optimization for different LIBS target composition, our new measurements qualitatively indicate that significant enhancements may be feasible and may enhance the use of LIBS for detection and identification of chemical compounds, biological species, and trace chemical films within a background matrix. It is important to note that the use of a CO₂ laser for enhancement is a technique that may have eye-safety advantages for stand-off applications; laser wavelengths greater than about 1.4 μm have several orders of magnitude greater maximum permissible exposure limits for direct ocular view.

It should also be noted that our two wavelength laser enhanced LIBS technique is similar to, but distinct from, previous work conducted using dual-pulse LIBS. For example, there has been extensive dual-pulse studies using both pre- and post-ablation secondary pulses which have shown enhancement using similar wavelengths for the dual pulses [5-8]. The use of a same wavelength double-pulse laser has been used for ablation of materials and enhancements in the plasma LIBS signal [9]. UV excimer and CO₂ lasers have been studied and used to enhance ablation of selected materials for thin film deposition [10], various dual-laser wavelengths investigated for LIBS enhancement [11], and a second resonant laser pulse has been used for resonance photoionization of the initial plasma discharge [12]. Our use of two different laser wavelengths at 1.06 μm and at 10.6 μm for LIBS is new, as far as we know, and serves to extend knowledge in LIBS enhancement using multiple laser sources.

2. Experimental apparatus

A schematic of our simultaneous dual-laser enhanced LIBS system is shown in Fig. 1.

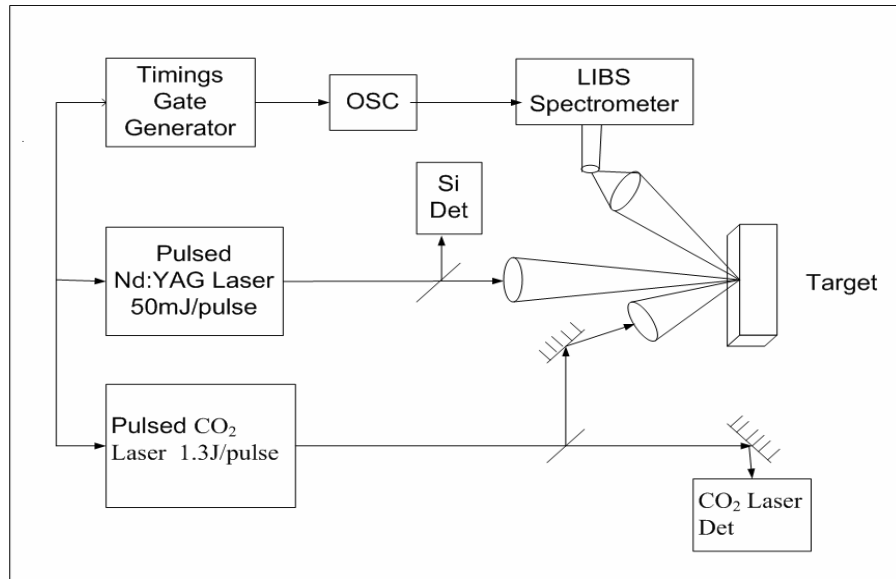


Fig. 1. Schematic of two laser LIBS system for CO₂ laser enhancement of Nd:YAG induced LIBS plasma emission

A Q-switched Nd:YAG laser (Big Sky Laser Model CRF200; 50 mJ/pulse, 5 Hz, 5 ns pulse length, $M^2 = 5$) was focused by a 10 cm focal length lens onto the target. The focused spot size was measured (by burn patterns) to be about 1 mm in diameter. The plasma produced on the target emitted LIBS emission into a 2π steradian solid-angle cone, which was collected using a 5 cm diameter lens (focal length of 10 cm) focused onto a fiber optic cable. The 300 micron core fiber optic cable transmitted the light to a spectrometer (Ocean Optics: Model HR2000; 200nm - 1100 nm) where it was detected by a linear photodiode array. An order-sorting filter in the spectrometer reduced second order features by a factor of 100 fold. The LIBS spectra from the spectrometer was then transferred to a notebook computer.

A high-power Q-switched CO₂ Transverse Electrode Atmospheric (TEA) laser (Lumonics Model 920; 1.3 J/pulse, 5 Hz) was used to produce 10.6 μm laser pulses that were then routed using mirrors onto the same LIBS emission target area. The pulse length of the CO₂ laser pulse had an initial TEA laser spike of 100 ns length followed by a nitrogen-fed tail about 5 μs long. The CO₂ laser output beam size was controlled using a lens to have a diameter on target between 3 mm to 15 mm. For a 6.5 mm diameter beam, the energy density was about 40 mJ/mm². The timing of the laser pulses was controlled with digital time-delay generators (SRS Model DG535), and the laser pulses were detected using fast Si photodiodes (Nd:YAG laser) and photon-drag detectors (CO₂ laser). A second high speed Si detector (not shown in Fig. 1) was placed within a few cm of the plasma and used to observe the total UV-visible emission from the LIBS plasma; this signal gave an indication of the intensity and temporal length of the plasma. The laser signals and respective timing overlap was displayed on a high-speed digital oscilloscope (LeCroy Model 940). The timing uncertainty (jitter) of the lasers was about 20 ns for the Q-switched YAG laser and about 500 ns for the TEA CO₂ laser. Timing errors of the gate electronics were negligible, on the order of a ns.

It should be added that the pulse-to-pulse stability of the YAG laser pulse energy was about 2% and about 5% for the CO₂ laser. The spatial profile of the YAG laser was

approximately a lower order top-hat mode and appeared stable in mode pattern. However, the Lumonics laser may have had a less stable spatial mode pattern due to small changes in the gain characteristics within the TEA discharge on a pulse-to-pulse basis.

The angular separation of the Nd:YAG beam and CO₂ beam was about 30 degrees, with the LIBS collection optics aligned at an angle of about 20 degrees from that of the Nd:YAG beam. The Nd:YAG laser beam was at near normal incidence to the sample.

Most of the data was taken using a high purity alumina target from CoorsTek (AD-998), which was 99.82% Al₂O₃. Listed impurities were: Na₂O 0.08%, MgO 0.07%, Fe₂O₃ 0.01%, and SiO₂ 0.02%.

3. LIBS measurements: Nd:YAG laser alone

An alumina ceramic target was used for our initial experiments since previous LIBS experiments had shown that alumina produces reproducible LIBS spectra. As such, Fig. 2 shows the LIBS emission measured using the Nd:YAG laser pulse alone. Figure 2 is for a single laser pulse; the statistical variability in the LIBS signal was approximately 15% for 100 laser pulses.

As can be seen, several LIBS lines are evident including two strong lines at 394.40 and 396.15 nm, most probably due to Al I (where the normal convention is used of I = neutral, II = singly ionized) [13]. These lines are just barely resolved by the portable spectrometer used for these initial results. Other Al I lines are observed at 308.22 and 309.27 nm (not resolved), 226.91 nm, 237.31 nm and 281.62 nm. There is also a weak Al II line at 422.68 nm. An Al II line at 281.62 nm is barely observable [13]. There is a trio of weak Mg I lines at 382.93, 383.23 and 383.83 nm which are not resolved. The broad line centered at 486.68 nm may be due to H I, although the line is broad and may be more molecular in nature. The line that at 517 nm is composed of three Mg I lines at 516.73, 517.27 and 518.36 nm. The strong line at 589 nm is actually the Na I doublet at 588.995 and 589.59 nm. The absolute error in the spectrometer wavelength reading was about 1 nm.

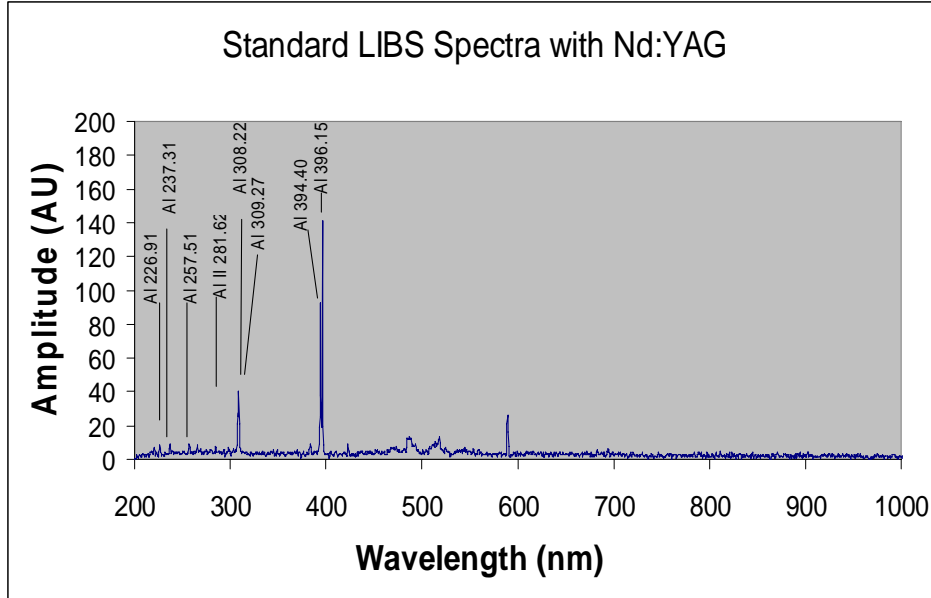


Fig. 2. LIBS signal from ceramic alumina target for Nd:YAG laser initiated plasma; emission lines are tentatively identified and listed in nm.

4. Enhanced LIBS measurements: Nd:YAG laser and CO₂ laser

The results with the addition of the CO₂ laser pulse are shown in Fig. 3; note that the intensity scale in Fig. 3 is about 25 times greater than that shown in Fig. 3. In addition to the previously observed lines, additional lines at 279.55 nm (Mg II); 358.66, 358.71 and 358.74 nm (Al II); 448.11 nm (Mg II); 466.31 nm (Al II); 559.32 nm (Al II); 622.62, 623.18 and 624.38 nm (Al II) from the substrate are observed. Note that all of these are +1 ions which were not often observed in the original Nd:YAG plasma. In the red and infrared region of the spectrum, several strong lines are observed, such as: H I at 656.27 and 656.29 nm (unresolved) or possibly molecular in nature; N I at 746.83 nm and O I at 777.19, 777.42 and 777.54 nm (unresolved). The latter lines may be related to atmospheric constituents, but further experiments would be required to differentiate this source from that due to the alumina target.

In order to ascertain the effect of the Nd:YAG laser power on the LIBS signal and make sure that the emission is linear with the plasma formed, Fig. 4 shows the LIBS signal of several of the prominent lines as a function of the Nd:YAG laser energy. Taking into account the errors (1 nm) in the spectrometer wavelength readings, we identified the emission lines in Fig. 4 as probably due to Al (237 nm), Mg II (279 nm), Mg (383 nm), Al (394 nm), and H (656 nm), although the latter line at 656 nm is rather broad and may be more molecular in nature.

As can be seen in Fig. 4, a threshold in the plasma formation or LIBS emission is observed at an energy of about 10 mJ (energy density of about 10 mJ/mm² for a beam area of 1 mm²). The emission intensity increases almost linearly with ND: YAG laser energy density above the threshold. This indicates that increasing the LIBS signal should be possible with increasing Nd:YAG laser power and that we were not saturating the Nd:YAG laser LIBS emission due to other possible effects such as quenching or target film ablation.

The influence of the CO₂ laser energy on the dual-laser LIBS emission was investigated for several neutral and singly ionized emission lines. Figures 5-7 show plots of the enhancement factor of the LIBS signal as a function of the CO₂ laser energy density for

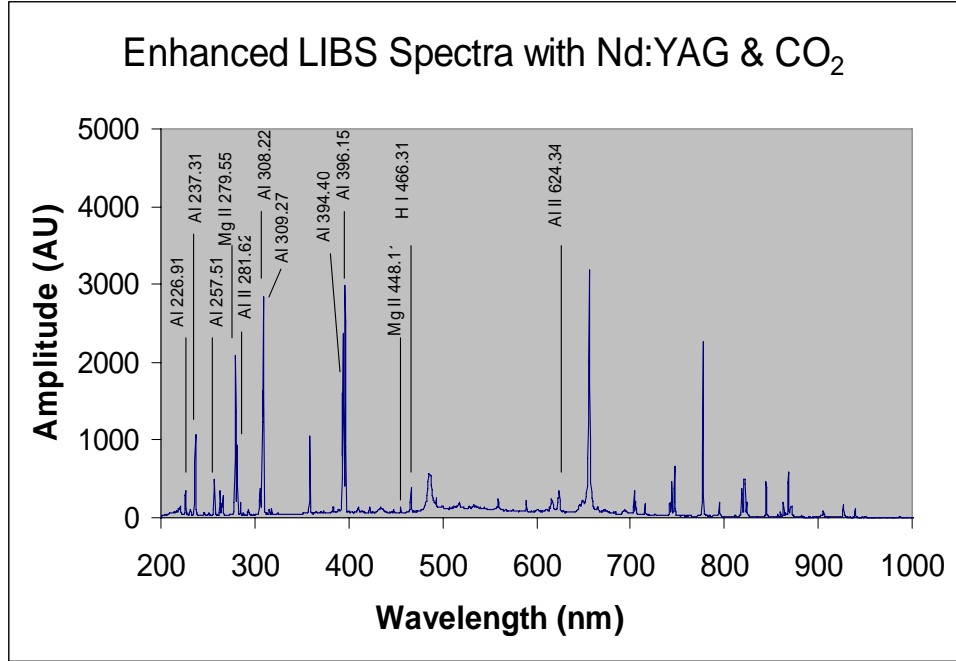


Fig. 3. LIBS emission signal for Nd:YAG laser initiated plasma and CO₂ laser enhancement

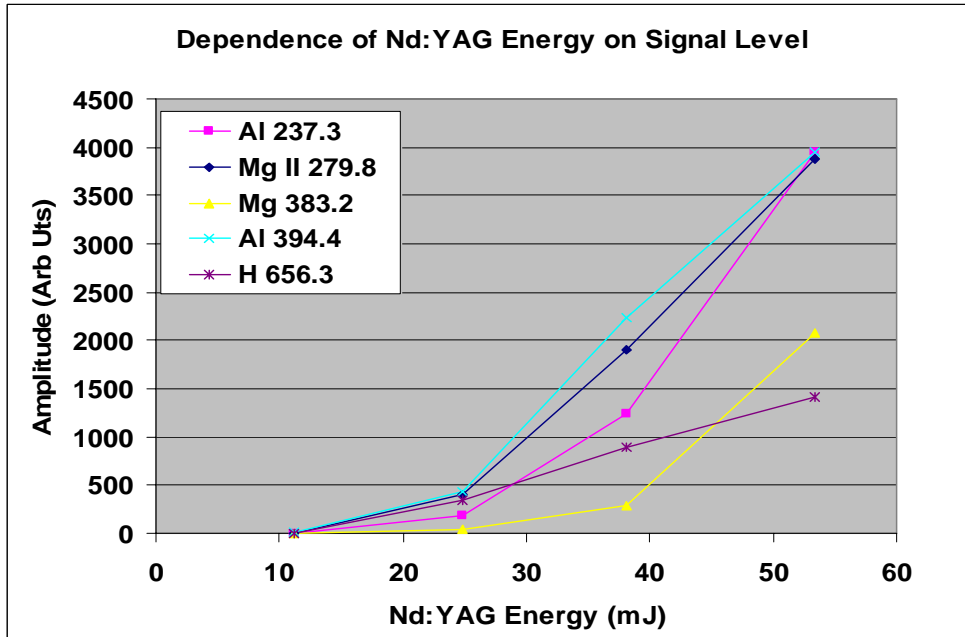


Fig. 4. LIBS signal for several emission lines (listed in nm) as a function of Nd:YAG laser energy (using Nd:YAG laser alone).

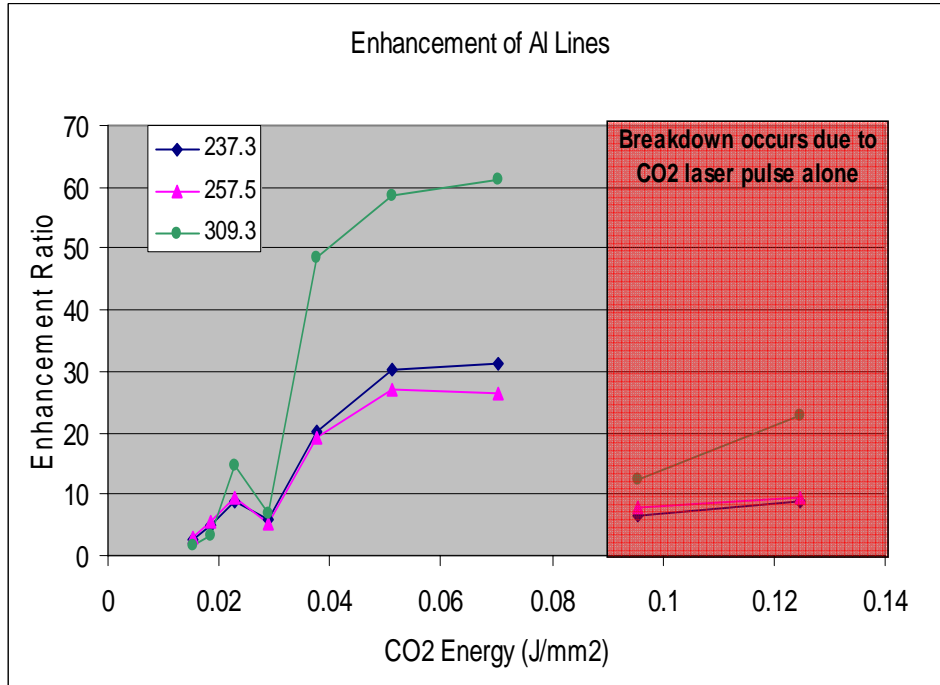


Fig. 5. LIBS enhancement ratio for Al LIBS lines (listed in nm) as a function of CO₂ laser intensity.

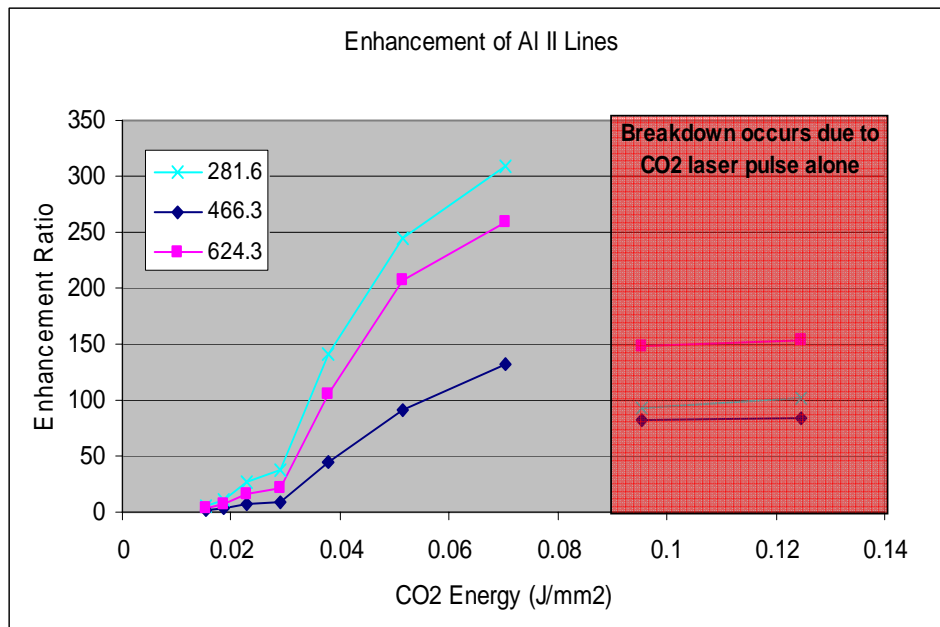


Fig. 6. LIBS enhancement ratio for Al II LIBS lines (listed in nm) as a function of CO₂ laser intensity.

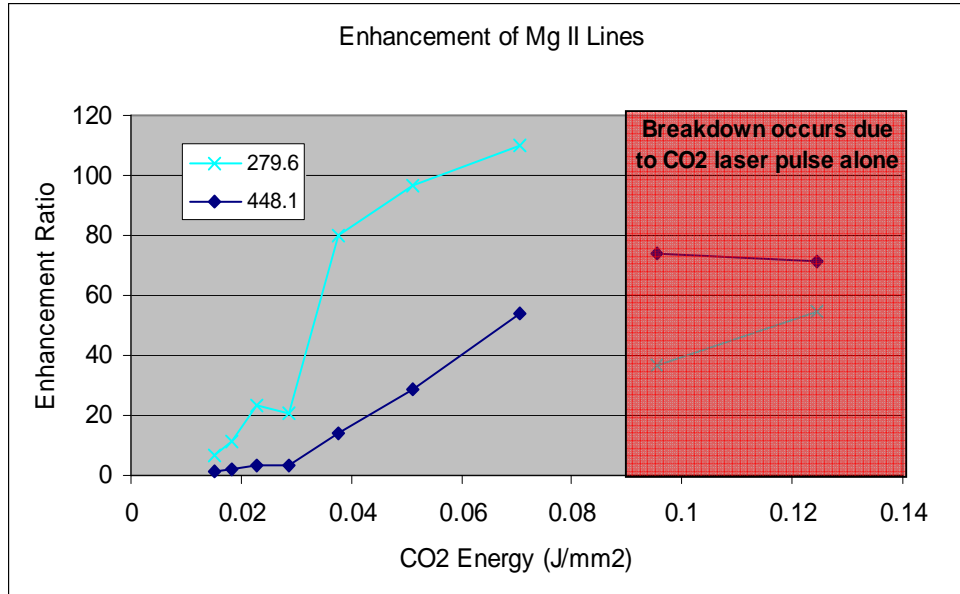


Fig. 7. LIBS enhancement ratio for Mg II LIBS lines (listed in nm) as a function of CO₂ laser intensity.

different selected emission elements and lines, where we have defined the LIBS enhancement factor as the ratio of the enhanced LIBS signal compared to the corresponding Nd:YAG LIBS signal after appropriate background (detector dark current) correction. It is important to note that, while the absolute accuracy in the line wavelengths was 1 nm, the identification of identical lines between the spectra in Fig. 2 and that in Fig. 3 for calculation of the enhancement ratio was much better, within about 0.1 nm, because the experimental geometry was sufficiently similar to allow the spectra to be directly compared.

Here, the Nd:YAG laser energy density was 50 mJ/mm² and the CO₂ laser was controlled using attenuators, aperture control, and lens focus to vary the energy density at the plasma location. As can be seen, the enhancement of the LIBS lines increases with CO₂ laser power, but only up to an energy threshold near 100 mJ/mm² where the onset of plasma formation due to the CO₂ laser alone was observed. The enhancement factor was found to be on the order of 25 to 300 times, depending upon the emission lines observed. For an alumina ceramic substrate the Al emission lines at 308 nm and Fe impurity line at 278 nm showed an increase of 60x and 119x, respectively. In addition, the enhancement of the LIBS lines was seen to vary, depending on which species was being observed, illustrating the need for additional study to determine the physical interactions, including ionization state coupling, on the plasma interactions. Overall, our data seems to indicate that the enhancement factor may be greater for the ionized states.

5. Timing overlap of two LIBS laser pulses

We investigated the timing overlap of the Nd:YAG laser and CO₂ laser pulse. For reference, Fig. 8 shows a plot of the scope trace of the CO₂ laser pulse (blue bottom trace) and the Nd:YAG laser pulse (upper green trace) for the case where the CO₂ laser pulse preceded the Nd:YAG plasma formation. In this case, no enhancement in the LIBS signal was observed.

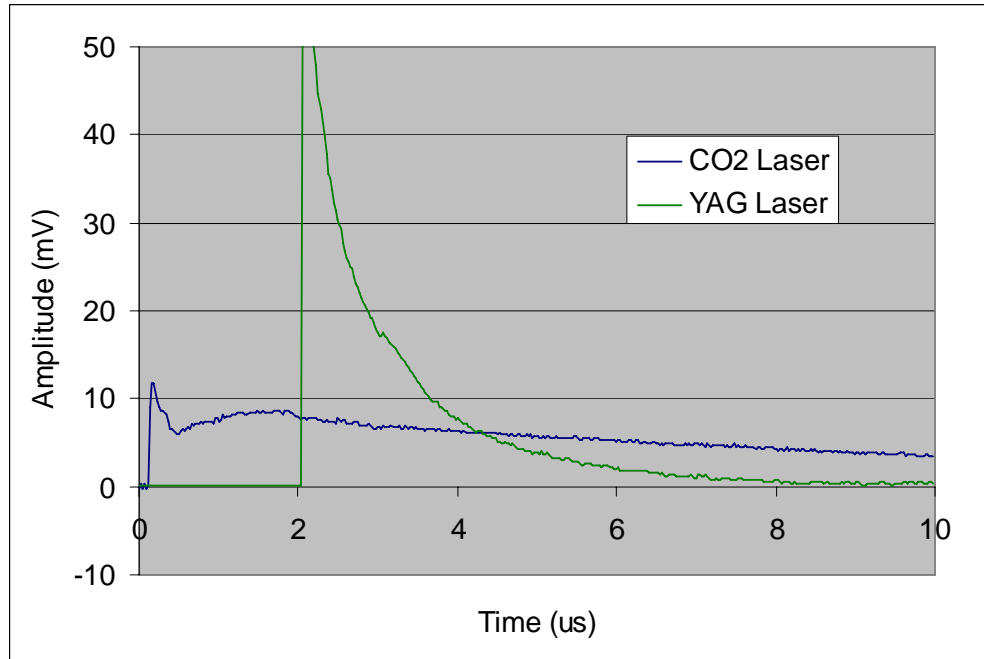


Fig. 8. Oscilloscope trace of Si detector (upper trace: Nd:YAG and plasma total emission) and CO₂ laser pulse (lower trace) when CO₂ laser leads Nd:YAG laser pulse. No enhancement in the LIBS emission was observed.

It should be noted that the upper Nd:YAG trace is from the Si photodetector which registers scattered Nd:YAG incident laser light and the UV and visible emission from the plasma. Subtracting the 5 ns Nd:YAG pulse, the plasma emission can be seen in the upper trace to have a lifetime ($1/e$) of about 1 μ s.

When the CO₂ laser pulse was delayed to more closely overlap the Nd:YAG induced plasma, then an enhanced LIBS emission was observed and the plasma emission was increased. This is seen in Fig. 9 which shows the same two laser pulses but with the CO₂ laser delayed to about 1/2 μ s after the initial Nd:YAG pulse.

The enhancement in the LIBS lines was measured as a function of the delay of the CO₂ laser pulse compared to the YAG laser pulse, and the results are shown in Fig. 10 for several of the LIBS lines. Significant enhancement occurred when there was between 0 to 0.5 μ s delay of the CO₂ pulse. However, as indicated earlier, there was timing jitter in controlling the CO₂ laser pulse on the order of 0.5 μ s. As can be seen, there are some differences in the enhancement for different emission lines, and further studies are being conducted to better quantify our results. It is important to note that the long tail of the CO₂ pulse is probably contributing to the enhancement effect, but further controlled studies are required using a short TEA CO₂ laser pulse with no tail to better determine how much of the enhancement is due to the CO₂ laser pulse heating the plasma to a higher temperature and how much of the enhancement is due to extending the lifetime of the plasma via the longer CO₂ pulse. We are planning to conduct these studies and will report on them in the future.

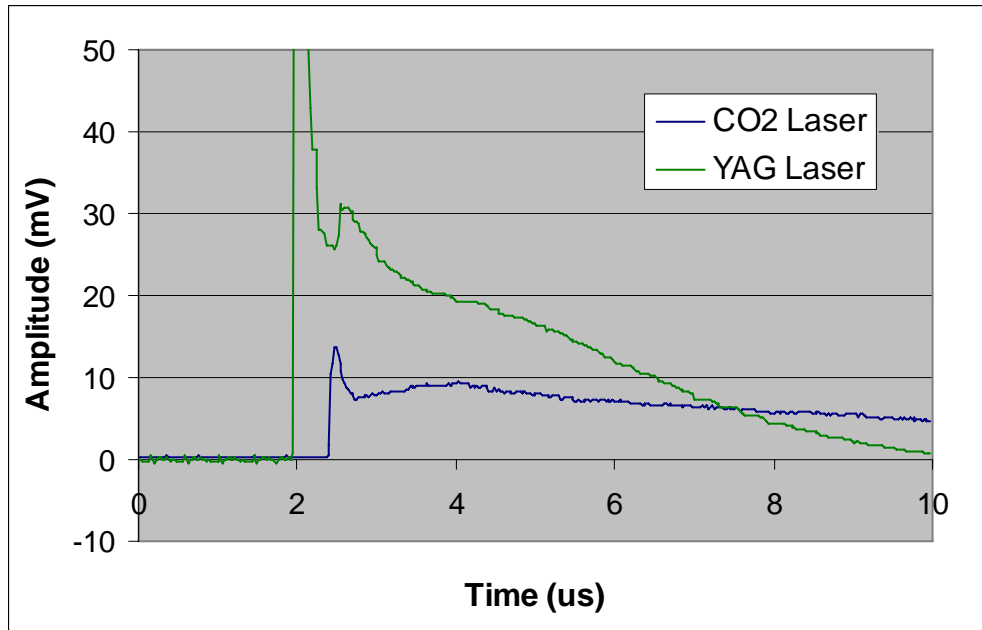


Fig. 9. Trace of Si detector and CO₂ detector for optimal overlap and LIBS enhancement.

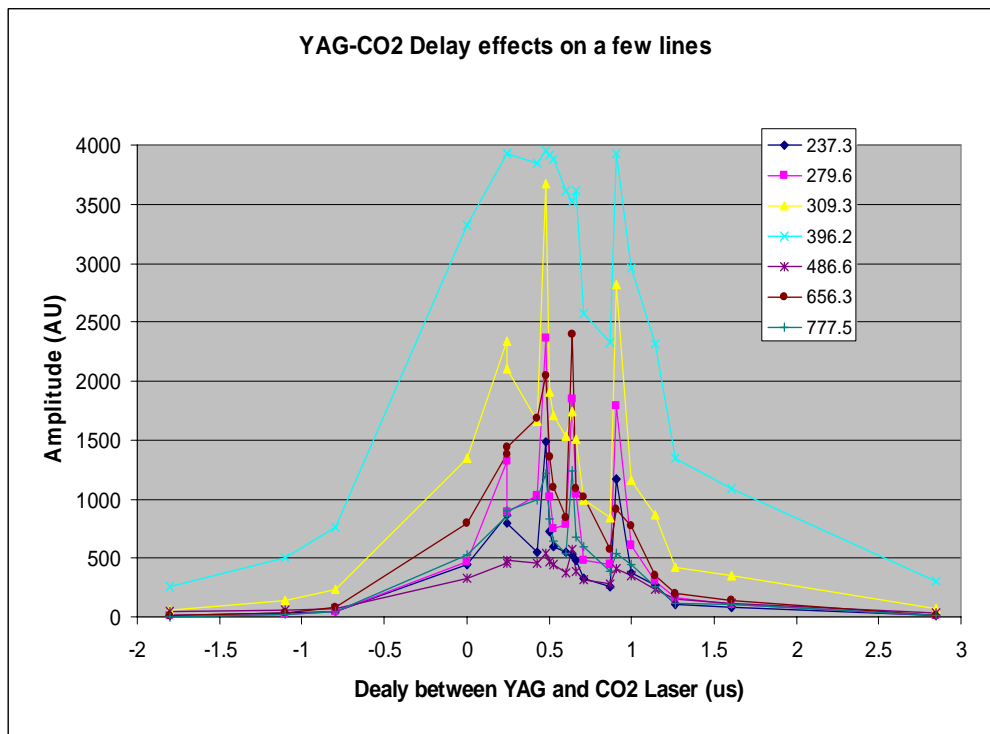


Fig. 10. Amplitude of LIBS emission lines (listed in nm) as a function of delay between ND:YAG and CO₂ laser pulses

6. Discussions and mechanisms

Our enhanced LIBS measurements give some qualitative indications of trends and preliminary insight into the mechanisms creating the enhancement. With some exceptions, enhancement of neutral atomic emission was usually on the order of 25 to 60 times, while enhancement of ionized species tended to be higher, 50 to 300 times. One of the exceptions is atmospheric gas components. Because they are not observed in high concentrations in the Nd:YAG only LIBS, any increase in concentration in the enhanced LIBS spectrum creates a significant enhancement factor.

We attribute the increase in both the neutral and the ionic emission to heating of the Nd:YAG plasma by the coincident CO₂ laser [2]. Such inverse bremsstrahlung absorption of CO₂ laser radiation in the free electrons of a plasma is well known in laser cutting and welding and can, in extreme cases, result in a "plasma mirror" attenuation of the incident CO₂ beam [2, 14-15]. While the exact mechanism occurring may be related to the inverse bremsstrahlung effect or a coupling to a Townsend discharge, we are conducting more detailed experiments to study the details of the enhanced emission process. It may be noted that inverse bremsstrahlung may be considered as a special case of the Townsend effect, which was discovered much earlier [16-18]. As such, we have chosen to call this particular enhanced LIBS process Townsend Effect Plasma Spectroscopy (TEPS), a term which helps to differentiate this two wavelength laser technique from regular single pulse LIBS, same wavelength dual-pulse LIBS, and fs and ns LIBS techniques.

As the delay experiments show, the enhancement is only in effect when the CO₂ laser has significant overlap with the Nd:YAG plasma, but can prolong the existence of the plasma significantly as shown in Fig. 10. In fact, the delay experiments show a convolution of the Nd:YAG and the CO₂ pulse profiles with a width of several microseconds, corresponding to a significant fraction of the CO₂ pulse duration.

In summary, we report for the first time the enhancement of LIBS intensities via coincident CO₂ laser irradiation with resulting increases of emission intensities of greater than two orders of magnitude in some cases. In addition, we are in the process of investigating and quantifying this enhancement factor using other target materials and will report on these results at a later date.

Acknowledgments

The research reported in this document/presentation was performed in connection with contract/instrument W911QX-07-C-0044 with the U.S. Army Research Laboratory under Prime Contract to Alakai Consulting & Engineering, Inc. The views and conclusions contained in this document/presentation are those of the authors and should not be interpreted as presenting the official policies or position, either expressed or implied, of the U.S. Army Research Laboratory or the U.S. Government unless so designated by other authorized documents. Citation of manufacturer's or trade names does not constitute an official endorsement or approval of the use thereof. The U.S. Government is authorized to reproduce and distribute reprints for Government purposes notwithstanding any copyright notation hereon."